Geologie en Mijnbouw **73:** 229–233, 1994.

A note on the foreshock of the 1992 Roermond earthquake, the Netherlands

Mihnea-Corneliu Oncescu[1], Thierry Camelbeeck[2] & Henri Martin[2]
[1] *Geophysical Institute, Karlsruhe University, Hertzstr. 16, 76187 Karlsruhe, Germany;* [2] *Royal Observatory of Belgium, Av. Circulaire 3, 1180 Bruxelles, Belgium*

Received 30 August 1993; accepted in revised form 15 December 1993

Key words: relative location, Roermons earthquake

Abstract

Vertical components from 12 digital seismic stations which recorded the $M_L = 5.8$ Roermond earthquake were used to determine the position and magnitude of a foreshock using relative methods. The small shock occurred 0.19 s before and 780 m away from the main shock on its SW-dipping fault plane. The local magnitude of the foreshock is $M_L = 4.0$, which corresponds to a seismic moment of $2.8 \cdot 10^{14}$ Nm and to a seismic energy of $4.3 \cdot 10^9$ J.

Introduction

The Roermond earthquake of April 13, 1992, at 01:20 UT with $M_S = 5.3$ ($M_L = 5.8$) was the largest earthquake in the Lower Rhine Embayment since the 1951 Euskirchen earthquake. Joi2nt hypocenter determination of the main shock and aftershocks using permanent and temporary stations (Camelbeeck et al. 1994) constrains the depth of the main shock to 17 km and allows the identification of the Peel Boundary Fault as the fault responsible for the earthquake. The focal mechanism corresponds to a pure dip-slip dislocation on a fault plane striking 124° and dipping 68° southwestward (Ahorner 1992, Paulssen et al. 1992, Braunmiller et al. 1994). The depth of the aftershocks ranges from 10.5 to 20 km.

The purpose of this note is to use arrival time differences and amplitude ratios of P-waves to determine the location and magnitude of a small foreshock of the Roermond earthquake. This foreshock was first identified by Ahorner (pers. comm., April 23, 1992). For the relative location of its hypocenter we used the 'master event' technique and for the relative magnitude determination the ratio of maximum velocities.

Data analysis

The data used in this study come from the permanent digital seismic stations in Belgium and the Grand-Duchy of Luxemburg, to which we added station Bochum (BUG) of the German Regional Station Network to cover an azimuth gap in the east. The station distribution relative to the main shock epicenter is presented in Fig. 1 and a list of the 12 stations we used is given in Table 1. This 'network' covers about 180° of azimuth, a fact that will render our determinations a reasonably degree of reliability.

The zoomed P-waves of the main shock at these 12 stations show that the main rupture phase was preceeded by a small foreshock (Fig. 2). The differences in arrival times were used in a 'master event' analysis in order to determine the relative position (and origin time) of the foreshock with respect to the main rupture phase. When picking the arrival time difference, we also looked at the theoretical travel time curves (Fig. 3). They show that we could expect complications in the 90–100 km epicentral distance interval, where the direct and refracted waves come closely in time. This epicentral distance corresponds approximately to that of stations CLA and BUG and we looked carefully how these two stations were fitted by the data.

The difference Δt at station i between the arrival times of waves radiated by two events 1 and 2 is given by

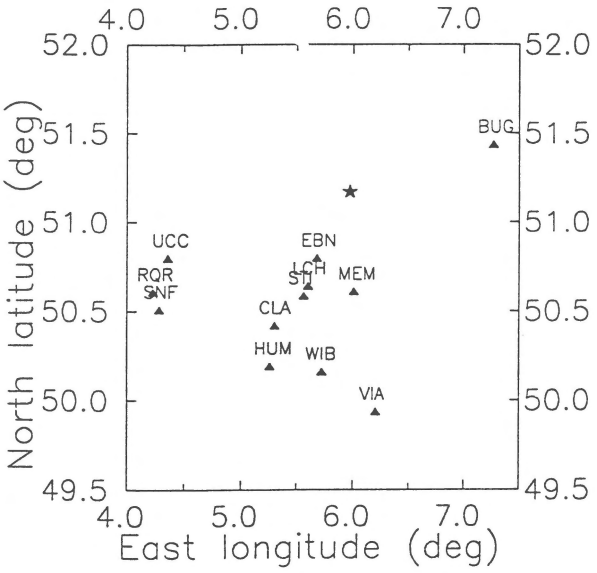

Fig. 1. Location of the 12 stations (▲) listed in Table 1 and the main shock epicenter (★).

$$\Delta t_i = t_o - (1/v_h)L\cos\gamma_i, \quad i = 1, \ldots, N \quad (1)$$

where t_o is the difference in origin times, L is the distance between the foci 1 and 2, v_h is the wave velocity in the focal region (in our application of P-waves at 17 km depth), γ_i is the angle between the ray leaving focus 1 and the direction connecting the two foci, and N the number of stations. Equation (1) is valid as long as the distances between the focal region and stations are much greater than distance L. In order to overcome the non-linearity of Equation (1) we conveniently re-write $L\cos\gamma_i$ as the scalar product of the vector **L** (starting in focus 1 and ending up in focus 2) with the unit vector e_i pointing in the ray-leaving direction. Thus, for N = 12 we find an overdetermined linear system of 12 equations

$$\Delta t_i = t_o - (l/v_h)\sum_{k=1}^{3} L_k e_{ik} \quad i = 1, \ldots, 12 \quad (2)$$

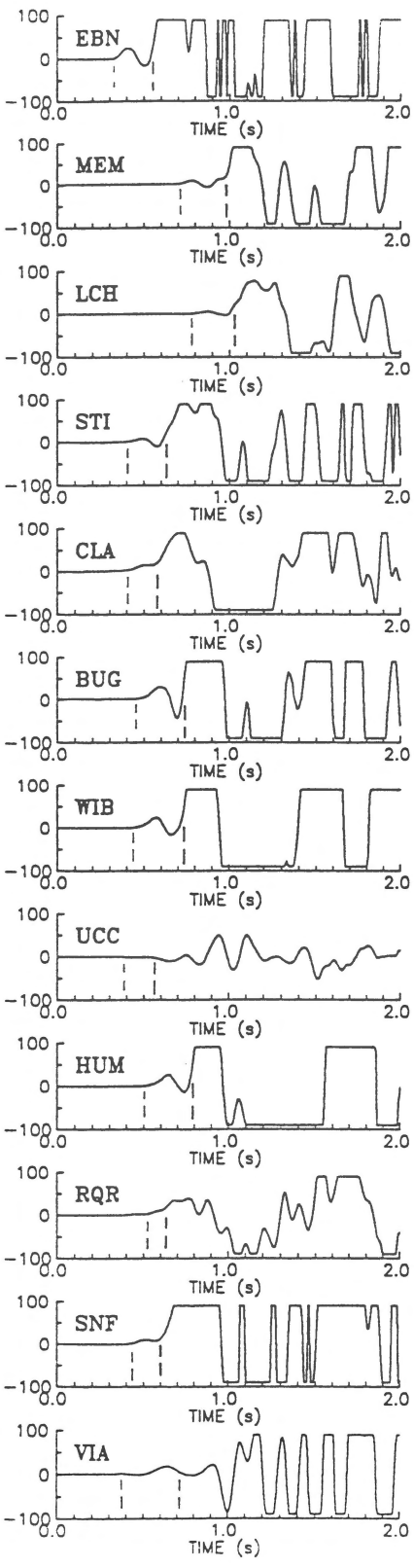

Fig. 2. P-wave trains in increasing order of epicentral distance displaying the foreshock signature. The units for the vertical axes are μm/s. Dashed lines mark the arrival time difference between foreshock and main shock. Data were clipped artificially except for those from stations EBN, CLA and SNF. For station codes and location see Table 1 and Fig. 1.

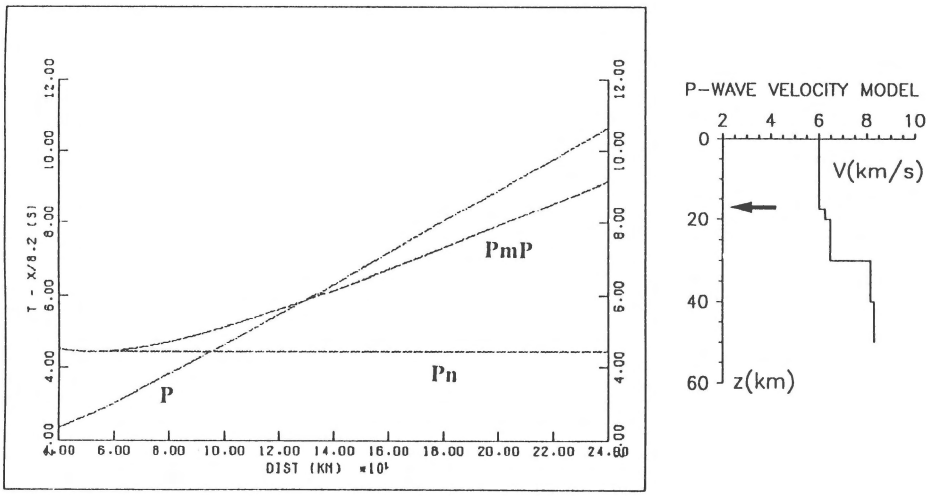

Fig. 3. Theoretical travel time curves (left) for the velocity model given at the right, depicting the direct wave (P), Moho-reflected wave (PmP) and Moho-refracted wave (Pn) branches. The arrow in the velocity model indicates the depth of the focus.

Table 1. List of stations used in the master event location analysis and magnitude determination for the foreshock of the 1992 Roermond earthquake

Station	Epicentral distance (km)	Azimuth α(°)	Take-off angle Θ (°)	Time difference Δ t (s)	Ratio of maximum ground velocities
EBN	46	203	110	0.224	12.7
MEM	64	176	105	0.240	15.5
LCH	65	202	105	0.248	13.4
STI	71	202	103	0.224	13.1
CLA	96	208	68	0.200	6.2
BUG	97	72	68	0.262	19.3
WIB	114	188	47	0.264	17.5
UCC	119	249	47	0.152	3.0
HUM	120	204	47	0.240	14.8
RQR	137	242	47	0.144	17.4
SNF	139	238	47	0.184	14.2
VIA	140	172	47	0.272	62.0

Table 2. Hypocenter and source parameters of the foreshock as determined from the reference parameters of the main shock adopted after Braunmiller et al. (1994) and Camelbeeck et al. (1994)

Parameters	Main shock	Foreshock
Origin time (UT)	01:20:03.10	01:20:02.91 ± 0.02
Latitude (°N)	51.170	51.174 ± 0.13 km
Longitude (°E)	5.970	5.961 ± 0.09 km
Depth (km)	17.0	16.9 ± 0.1
Seismic moment M_0 (Nm)	$8.3.10^{16}$	$(2.8 \pm 1.1).10^{14}$
Local magnitude M_L	5.8	4.0 ± 0.4
Source radius r (km)	2.1	0.5 ± 0.1
Brune stress drop $\Delta\sigma$ (MPa)	4.1	1.3 (tentatively)

with 4 unknowns, i.e. t_o, L_1, L_2 and L_3. L_k are the vector components of **L** indicating the relative distances along NS, EW and downward axes. The components of e_i are given by $e_{i1} = \sin\Theta_i\cos\alpha_i$, $e_{i2} = \sin\Theta_i\sin\alpha_i$ and $e_{i3} = \cos\Theta_i$, where Θ_i is the take-off angle and α_i is the azimuth as listed in Table 2. We used v_h = 6 km/s. Equation 2 was solved using a classical least-squares approach and the standard errors of the four unknowns were propagated to all derived results. Figure 4 displays the obtained linear dependence between Δt_i and $\cos\gamma_i$ according to Equation 1. The observations at stations CLA and BUG do not deviate from the trend of the data and do not change the results when removed.

From the components L_k we then computed the distance between the two foci, $L = (L^2_1 + L^2_2 + L^2_3)^{1/2}$, then the azimuth ϕ and the dip δ of foreshock position relative to the mainshock hypocenter are: ϕ = arctan (L_2/L_1) respectively δ = arccos (L_3/L). The foreshock occurred 0.19 ± 0.02 s before the main shock at a distance L = 780 ± 110 m in a direction given by an

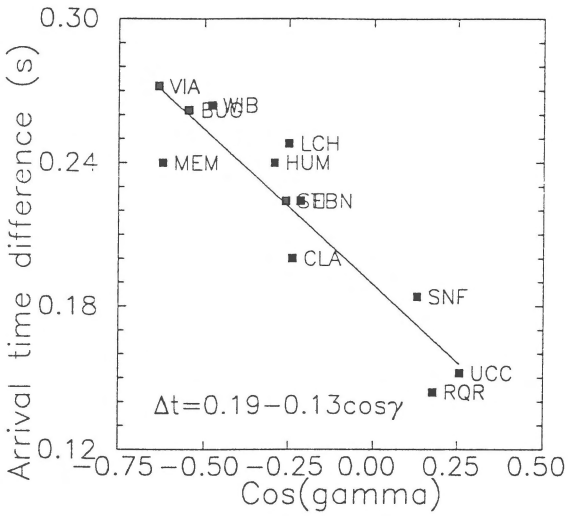

Fig. 4. The measured arrival time differences Δt_i (■) are a function of $\cos\gamma_i$ and the obtained linear fit (line) according to the method described in the text. For station codes and location see Table 1 and Fig. 1.

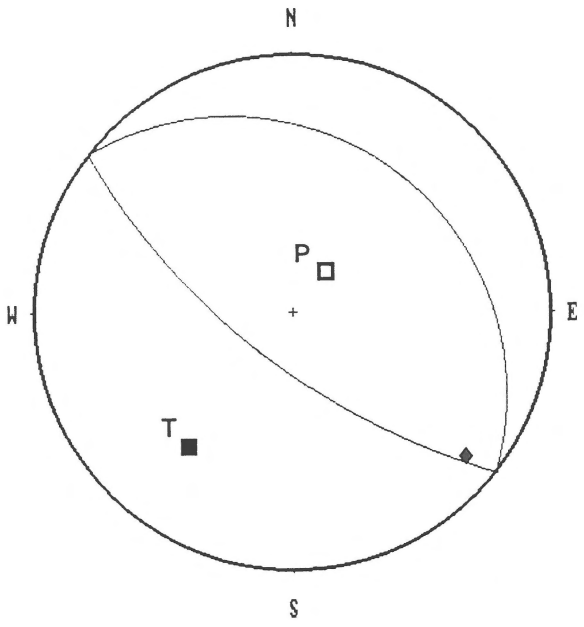

Fig. 5. Vector **L** (♦) indicating the position of the foreshock on the fault-plane solution for the main shock as obtained by Ahorner (1992). Stereographic projection on the lower hemisphere. P: compressional axis, T: tensional axis.

azimuth of 310° ± 9° and a dip of −8° ± 7° (a negative dip means above the local horizon). Vector **L** indicating the position of the foreshock is presented in Fig. 5 on the fault-plane solution of Ahorner (1992). The foreshock is situated on the SW-dipping nodal plane, offering an unambiguous identification of the actual rupture plane. The same choice was made from seismotectonic reasons by Ahorner (1992) and Pelzing (1992) and from aftershock distribution by Camelbeeck et al. (1994).

To infer the magnitude of the foreshock we applied also a relative method. We measured the ratio of maximum ground velocities V_2/V_1 from the vertical component P-wave trains, where the indices 1 and 2 refer to the foreshock and main shock, respectively. Then, for a magnitude scale of the form $M_L = \log A + b$, where A is the maximum ground displacement usually within the S-wave train, and assuming that the S-wave amplitude ratio equals the P-wave amplitude ratio (the same focal mechanism for both shocks), we find:

$$M_{L2} - M_{L1} = \log(V_2/V_1) + \log(f_1/f_2) \quad (3)$$

Here we used that $A = V/2\pi f$, where f is the predominant frequency in the signal. We adopted a value f_2 = 1 Hz for the main shock (Ahorner 1992, Braunmiller et al. 1992) and f_1 = 4.5 Hz for the foreshock as the inverse of the mean 'time difference' in Table 1.

In the magnitude determination, we rejected station VIA due to its strong site response (Oncescu et al. 1994). The average ratio of maximum ground velocities was 15.3 ± 2.2, resulting in a magnitude difference of 1.8 ± 0.2 units. Consequently, with M_{L2} = 5.8 (Camelbeeck et al. 1994) we find M_{L1} = 4.0 ± 0.2 (or ± 0.3 if one takes M_{L2} = 5.8 ± 0.2). We believe that an estimate of f_1 may range between 3.5 and 6 Hz, i.e. an error factor of 1.3. Considering also this uncertainty we finally arrive at a magnitude estimate of M_{L1} = 4.0 ± 0.4. So, the foreshock is larger than the largest aftershock!

Extrapolating the empirical relationships obtained by Oncescu et al. (1994), $\log M_o$ (Nm) = 1.02 M_L + 10.36 and $\log E_S$(J) = 1.90 M_L − 17.8 for exactly the same region but for the magnitude interval M_L = 1.9–3.4, we arrive at an estimate of the seismic moment $M_o = 2.8 \cdot 10^{14}$ Nm and the released seismic energy $E_s = 4.3 \cdot 10^9$ J for the foreshock. If we further adopt the predominant frequency f_1 = 4.5 Hz as the P wave corner frequency of the foreshock, we obtain an estimate for its source radius, r_1, and stress drop, $\Delta\sigma_1$, relative to the main shock using the relations:

$$r_1/r_2 = f_{c2}/f_{c1} \text{ and } \Delta\sigma_1/\Delta\sigma_2 = (M_{o1}/M_{o2})(r_2/r_1)^3 \quad (4)$$

From the main shock source parameters (Braunmiller et al. 1992) we obtain the results given in Table 2. The standard error of $\Delta\sigma$ was not determined due to the very strong dependence on radius, i.e. f_1 estimate. Therefore $\Delta\sigma$, should be considered with caution.

Final remarks

The determined foreshock position further corroborates the rupture plane as being the one dipping 68° southwestward. One may speculate that the main rupture phase started on the same fault plane, but at the margin of the foreshock rupture zone, as the relative distance of 780 $\pm$ 110 m is comparable with the foreshock source radius of about 500 m. The foreshock magnitude is approximately two units smaller than the main shock magnitude.

Acknowledgements

We thank K. Bonjer and R. Verbeiren for encouraging this study and for critically reading the manuscript. Two anonymous reviewers helped with their comments. We also thank T. van Eck for accepting a late contribution. This study has been supported by the German Research Association (SFB 108), by the IDNDR Project of the University of Karlsruhe and by the Royal Observatory of Belgium.

References

Ahorner, L. 1992 Das Erdbeben bei Roermond am 13. April 1992 and die daraus zu ziehenden Lehren für das Erdbebengafährdungspotential im Rheinland – Mitt. Deutsch. Geophys. Ges. 1–2/1992: 51–57

Braunmiller, J., K.P. Bonjer, T. Dahm, M.C. Oncescu & T. Plenefisch 1992 Das Roermond-Erdbeben vom 13.4.1992 – erste Ergebnisse unter Benutzung von Daten des German Regional Seismic Network (GRSN) und des digitalen Netzes im Oberrheingraben – Extended Abstract; presented at the Annual Meeting of the Working Group Gräfenberg, 27–28 May 1992, Bad Königstein

Braunmiller, J., T. Dahm & K.P. Bonjer 1994 Source mechanism of the 1992 Roermond earthquake from surface wave inversion of regional data – Geophys. J. Int. 116: 663–672

Camelbeeck, T., T. van Eck, R. Pelzing, L. Ahorner, J. Loohuis, H.W. Haak, P. Hoang-Trong & D. Hollnack 1994 The 1992 Roermond earthquake, the Netherlands, and its aftershocks – Geol. Mijnbouw, this issue

Oncescu, M.C., T. Camelbeeck & H. Martin 1994 Source parameters for the Roermond aftershocks of April 13–May 2, 1992 and site spectra for P and S waves at the Belgian seismic network – Geophys. J. Int. 116: 673–682

Paulssen, H., B. Dost & T. van Eck 1992 The April 13, 1992 earthquake of Roermond (The Netherlands); first interpretation of the NARS seismograms – Geol. Mijnbouw 71: 91–98

Pelzing, R. 1992 Das Erdbeben von Roermond 13. April 1992 – Publ. Geol. Landesamt Nordrhein-Westfalen, 16 pp